

The Gross Architecture of an Antibody-Combining Site as Determined by Spin-Label Mapping

By BRIAN J. SUTTON,* PETER GETTINS,* DAVID GIVOL,† DEREK MARSH,*‡
SIMON WAIN-HOBSON,* KEITH J. WILLAN* and RAYMOND A. DWEK*

*Department of Biochemistry, University of Oxford, South Parks Road, Oxford OX1 3QU, U.K., and

†Department of Chemical Immunology, Weizmann Institute of Science, Rehovot, Israel

(Received 26 October 1976)

1. A series of Dnp (dinitrophenyl) nitroxide spin labels was used to map the dimensions of the combining site of the Dnp-binding immunoglobulin A myeloma protein MOPC 315. The method compares the observed e.s.r. (electron-spin-resonance) hyperfine splittings with those calculated on the basis of different postulated motions for the spin label. The analysis is complicated by the sensitivity of the e.s.r. hyperfine splitting to the overall 'tumbling' time of the antibody-hapten complex and the polarity of the spin-label's environment. When these effects are considered quantitatively, it is then possible to determine the degree of mobility of each hapten which is allowed by the shape of the combining site. 2. The dinitrophenyl ring is rigidly held, and the depth of the site is 1.1-1.2 nm and has lateral dimensions at the entrance to the site $\geq 0.6 \text{ nm} \times 0.9 \text{ nm}$. The analysis of the results for spin-labelled haptens with chiral centres allows these lateral dimensions to be refined to 0.8 nm and 1.1 nm, and it is shown that the site is asymmetric with respect to the plane of the dinitrophenyl ring. 3. A polarity profile of the combining site was also obtained and a positively charged amino acid residue, possibly arginine-95_L (light chain), was located at the entrance to the site. 4. The binding of Gd(III) to the antibody-hapten complexes results in quenching of the e.s.r. signal of the nitroxide. By using La(III) as a control, the paramagnetic contribution to the quenching is measured. 5. Analysis of the differential quenchings of the enantiomers of two five-membered nitroxide ring spin labels gives two possible locations of the metal-binding site. One of these is equidistant (0.7 nm) from each of the three dinitrophenyl aromatic protons, and nuclear-magnetic-resonance relaxation studies, at 270 MHz, on solutions of dinitrobenzene, Gd(III) and the Fv fragment (variable region of heavy and light chain) from protein MOPC 315 support this location for the metal site. 6. The e.s.r. and metal-binding data were then compared with the results of a model of the combining site constructed on the basis of framework invariance in immunoglobulins [Padlan, Davies, Pecht, Givol & Wright (1976) *Cold Spring Harbor Symp. Quant. Biol.* 41, in the press]. The overall agreement is very good. Assignments of possible chelating groups for the metal can be made.

The method of e.s.r.§ mapping was developed by Hsia & Piette (1969) and is based on the effects of molecular motions on the e.s.r. spectrum of the nitroxide free-radical group. Hsia & Piette (1969) prepared a series of Dnp-spin-labelled haptens in which they systematically increased the chain length separating the haptenic group from the nitroxide, and

‡ Permanent address: Max-Planck-Institut für Biophysikalische Chemie, D-3400 Göttingen, W. Germany.

§ Abbreviations: e.s.r., electron spin resonance; n.m.r., nuclear magnetic resonance; Dnp, dinitrophenyl; IgA, immunoglobulin A; Fab fragment, N-terminal half of heavy chain and light chain; Fv fragment, variable region of heavy and light chain; Pipes, 1,4-piperazinediethanesulphonic acid. Subscript H or L after residue numbers refers to the heavy and light chain respectively.

thus estimated the depth of the combining site in rabbit anti-dinitrophenyl antibodies to be between 1.1 and 1.2 nm. It has to be assumed that the dinitrophenyl acts as the 'anchor' in the combining site for these haptens. If the nitroxide group of these haptens is within the combining site and cannot move independently of the antibody, it will display an e.s.r. spectrum characteristic of the antibody 'tumbling' rate. At the other extreme, when the nitroxide group is outside the combining site, it will have a mobility independent of the antibody and an e.s.r. spectrum similar to that of a free spin label.

The specificity of mouse myeloma protein MOPC 315 IgA for dinitrophenyl ligands suggests that the dinitrophenyl ring here will act as a suitable anchor grouping. The geometry and flexibility of the

combining site in protein MOPC 315 have been probed by using Dnp-spin-labelled haptens of different lengths (Dwek *et al.*, 1975*a,b*), but it was pointed out that the approach described above can be made more rigorous and extended by considering the likely anisotropic motions of the spin labels. The method consists of comparing the observed e.s.r. spectra with those expected on the basis of different possible motions for the spin label. This enables the extent of the mobility of the labels to be determined. Since the constraints on this mobility are conferred by the shape of the combining site, the motion of the label provides information about the geometry of the site. The analysis is complicated by the additional sensitivity of the e.s.r. spectra to the overall tumbling rate of the protein and also to the polarity of the label's environment, but both these factors can be taken into account. Although various methods exist for probing the depth of the site, the e.s.r. method is the only one that can also provide the lateral dimensions in solution. These may be particularly important in comparing different proteins that bind the same ligand or hapten. Of particular importance in the work described here is the use of five-membered nitroxide ring spin-labelled haptens which have chiral centres, for such haptens also allow the asymmetry of the site to be probed.

The concept of framework invariance in immunoglobulins is now established (Poljak, 1975; Padlan *et al.*, 1976). The implications of this are that it is feasible to construct, by using the known structures of immunoglobulins, the binding sites of new immunoglobulins on the basis of their sequence only. This has been carried out for the Dnp-binding protein MOPC 315 (Padlan *et al.*, 1976), but further physical information is required to confirm this structure.

The e.s.r. spectrum of a Dnp-spin-labelled hapten is quenched by Gd(III) and this allows the determination of metal-nitroxide distances (Dwek *et al.*, 1976). The use of a series of spin labels allows several independent determinations of metal-nitroxide distances to be obtained, with consequent location of the metal.

Correlation of the metal binding data with the model allows assignment to be made of the groups on the protein involved in chelating the metal.

Materials and Methods

Preparation of IgA, Fab and Fv fragments from protein MOPC 315

IgA was prepared from the serum of tumour-bearing mice (Inbar *et al.*, 1972); the Fab fragment was prepared by peptic digestion of IgA and the Fv fragment by further peptic digestion of Fab fragment (Hochman *et al.*, 1973). The protein was freeze-dried and stored at -20°C .

Spin labels

The series of spin-labelled haptens was prepared by the methods of Stryer & Griffith (1965), Hsia & Piette (1969) and Dwek *et al.* (1975*a*). In view of their limited solubility in water, ethanol was used, but was always $\leq 5\%$, in solutions containing protein. Haptens (V) and (VI) (Table 2) were both used as an unresolved mixture of the two enantiomers.

Metal ions

Solutions were prepared by heating the oxides (99.9% pure; Koch-Light Laboratories, Colnbrook, Bucks., U.K.) in air at 600°C and dissolving them in HCl. The pH was adjusted to 5.5–6.0 with NaOH, and concentrations were checked by titration with EDTA, with Eriochrome Black T as indicator.

Electron spin resonance

E.s.r. spectra were recorded on a Varian 109 (E-line) spectrometer operating at X-band (9.5 GHz) at room temperature (20°C). Samples were contained in a flat cell with a syringe attachment for mixing. This arrangement allows titrations to be carried out without disturbing the instrumental settings. All measurements are corrected for dilution. All spectra were recorded under non-saturating conditions, with a modulation amplitude of 0.2 mT. Protein samples (determined by using $A_{280}^{1\%} = 15.0$) were 50–100 μM in 0.15 M-NaCl/0.05 M-Pipes buffer, pH 6.4. The hyperfine-splitting constants measured from the e.s.r. spectra, and given in the Tables, are quoted with limits that indicate the precision with which the centres of the peaks may be located.

Nuclear magnetic resonance

N.m.r. spectra were recorded at 270 MHz in a Bruker spectrometer (Fourier-transform model) and Oxford Instrument Co. (Osney Mead, Oxford, U.K.) super-conducting magnet.

Samples of Fv fragment were at a concentration of 1.2 mM in 99.8% $^2\text{H}_2\text{O}$ (Ryvan Chemicals, Botley Rd., Southampton, U.K.) with 0.15 M-NaCl. Experiments were carried out at 303 K. Chemical shifts are reported as p.p.m. downfield from the sodium salt of 3-(trimethylsilyl)propanesulphonic acid, as external standard.

Computer visual display: determination of the mobility of five-membered nitroxide ring spin-label haptens

By using the SOFAR3 program (Dr. L. Ford, Laboratory of Molecular Biophysics, Department of Zoology, University of Oxford, Oxford, U.K.) available on the ARGUS 600 computer in the Laboratory of Molecular Biophysics, visual displays of the two

spin-labelled haptens (V) and (VI) (see Table 4) were generated and manipulated to determine the degree of motion allowed around certain single bonds without involving unfavourable van der Waals interactions. For this, molecular models were built of each of the haptens [by using CRE (Cambridge Repetition Engineers) components] and the atomic co-ordinates determined from these.

Having specified the covalent bonds in each molecule and the van der Waals radii for each type of nucleus, the programme indicates unfavourable interactions, given by separations of less than the sum of their van der Waals radii, by displaying a dotted line joining the two nuclei. Thus the most favourable conformations have no dotted lines indicated on the visual display.

Determination of the mobility of other haptens

For the other haptens, with more rotatable bonds and greater separation between the bulky alicyclic and aromatic rings, there was considerably greater freedom of movement than with the above two five-membered spin labels. Therefore mobilities were determined from CRE models, to which had been added space-filling components (Courtaulds, from Ealing Scientific, Watford, Middx., U.K.) on the same scale, to represent the van der Waals sphere.

Theory

A series of nitroxide ring spin labels was used to map the combining site of protein MOPC 315. Each label contains either a five- or six-membered nitroxide ring connected to the dinitrophenyl ring by a variable group (X) [5(SL) and 6(SL) respectively] (see the formulae).

The dinitrophenyl is the 'anchor' group, and the mapping is carried out by systematically varying X. It is assumed that the mode of binding of the dinitrophenyl is the same for all haptens.

The method involves quantification of the effect of the slow tumbling of the protein-hapten complex, in order that the contribution to the observed e.s.r. spectrum from motion of the spin-labelled hapten relative to the protein (within the combining site) may be determined. The effect of slow tumbling can be quantified, since the IgA, the Fab and Fv fragments form a set of molecules with the same binding

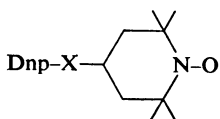
site but different rates of overall tumbling, as a result of their different molecular weights. In addition, polarity effects on the hyperfine coupling constant can give extra information about the nature of the site.

Effect of motion on the e.s.r. spectrum

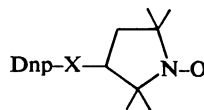
The nitroxide radical, with its conventional co-ordinate system, is shown in Fig. 1(a). In an oriented crystal the e.s.r. spectra obtained when the applied magnetic field (H) is directed along each of the three axes show three lines in each case, but their separation depends on the orientation. These three lines result from the interaction between the unpaired electron spin and the magnetic moment of the ^{14}N nucleus, characterized by the hyperfine-splitting constant A . The components of A in the x , y and z directions are shown in Figs. 1(b)–1(d), and are termed the principal values. Typical values of these are $A_{zz} = 3.2\text{mT}$, $A_{xx} = A_{yy} = 0.6\text{mT}$ (Griffith *et al.*, 1965), which demonstrate that, for this radical, the A tensor has axial symmetry.

For a random distribution of orientations, in a rigid glass, the observed spectrum is the sum of the spectra (b)–(d) in Fig. 1 together with those from all intermediate orientations (Fig. 1e). This spectrum is also obtained for any sample of randomly oriented spin labels, provided they have no molecular motion fast enough to be detected by e.s.r. Furthermore the splitting between the outer extrema (denoted $2A_{z'z'}$; Fig. 1e) approximates closely to $2A_{zz}$. If, however, the label is mobile and tumbles isotropically, the anisotropy in A is averaged and three sharp lines result, as shown in Fig. 1(f) (typical of a spin label free in solution). The spectra in Figs. 1(e) and 1(f) are the extremes of slow and fast (isotropic) motion.

The e.s.r. spectrum also depends on the degree of anisotropy of the motion. A spin label bound to a macromolecule undergoes two types of motion: slow isotropic tumbling of the whole complex and a faster, in general anisotropic, motion relative to the macromolecule. These occur at very different rates and are assumed to be uncoupled, and are therefore treated separately. The possibility of slower motion of the hapten relative to the protein has also been considered (see the Results and Discussion section), but the results indicate that this is not occurring.



Six-membered nitroxide ring spin label 6(SL)



Five-membered nitroxide ring spin label 5(SL)

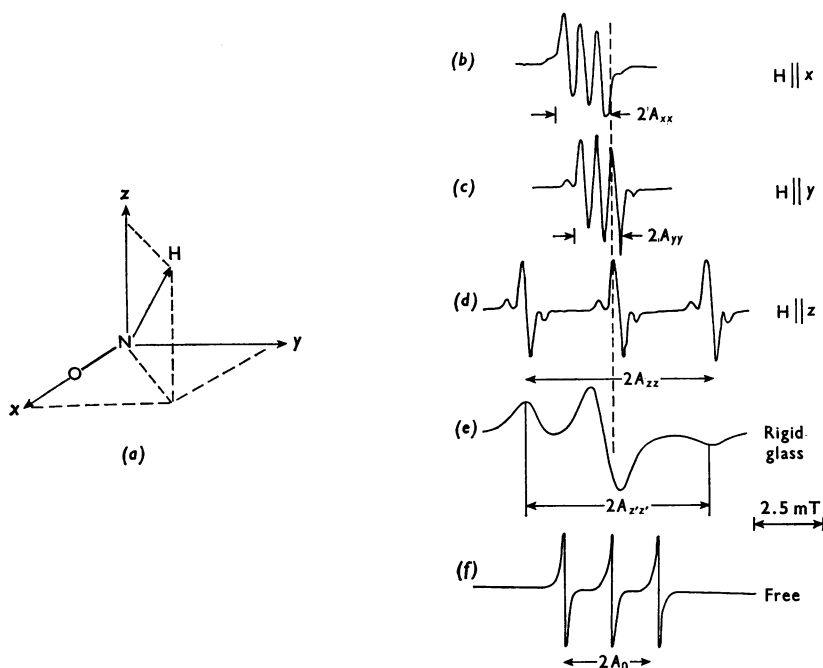


Fig. 1. Characteristics of e.s.r. spectra of the nitroxide radical

(a) The nitroxide radical co-ordinate system. (b)–(d) show the 9.5 GHz e.s.r. spectra obtained from the nitroxide radical oriented in the magnetic field as indicated. The rigid-glass spectrum (e), which is the sum of the spectra (b)–(d) and all intermediate orientations, represents the spectrum obtained for a sample of randomly oriented spin labels which have no molecular motion fast enough to be detected by e.s.r. Spectrum (f) represents that of a spin label freely mobile in solution.

Slow isotropic motion

The sensitivity of the e.s.r. spectrum of a spin label to rotational motion (characterized by a correlation time τ_r) has been well documented (Freed, 1976) for values of τ_r in the range 10^{-9} s $< \tau_r < 10^{-7}$ s. Outside this range the spectrum approaches a 'fast limit', the three-line spectrum in Fig. 1(f), and a 'slow limit', the rigid-glass spectrum in Fig. 1(e). For the IgA and antibody fragments used here τ_r lies within the range 5×10^{-9} – 5×10^{-8} s. The spectral feature most readily correlated with τ_r is the splitting between the outer extrema ($2A_{z'z'}$), which decreases as the rate of tumbling increases. Computer simulations of e.s.r. spectra (McCalley *et al.*, 1972) have related the difference in positions of the high- and low-field peaks from those in the rigid-glass spectrum with the value of τ_r . This established an empirical relationship between the observable $A_{z'z'}$ and τ_r . Thus, if τ_r can be calculated, e.g. from the Stokes–Einstein relation (Dwek *et al.*, 1975b), any differences between the expected splitting of the outer extrema and the observed splitting may indicate other motional effects. The relationship between τ_r and $A_{z'z'}$ allows the effect of the tumbling of the complex

on the spectrum to be calculated. The subsequent analysis of the faster anisotropic motion of the label relative to the protein can then be assessed.

Fast anisotropic motion

This motion is assumed to be fast on the e.s.r. time scale ($\leq 10^{-9}$ s), so that the effect is to average the principal values of the A tensor giving a new hyperfine tensor $\langle A \rangle$ with different principal values. For example, if the spin label undergoes a fast bond rotation, such that the nitroxide radical rotates about the x axis, A_{yy} and A_{zz} will be averaged and A_{xx} left unchanged. $\langle A \rangle$ will be axially symmetrical, but now the maximum component value of A will be 1.9 mT, the average of the A_{yy} (0.6 mT) and A_{zz} (3.2 mT) values. If A is axially symmetrical and characterized by principal values $A_{xx} = A_{yy} \neq A_{zz}$, an inner splitting of the spectrum may be observed, and all three principal values can be determined.

Motional averaging calculations

To calculate the effect of anisotropic motion on the e.s.r. spectrum it is necessary for the motion

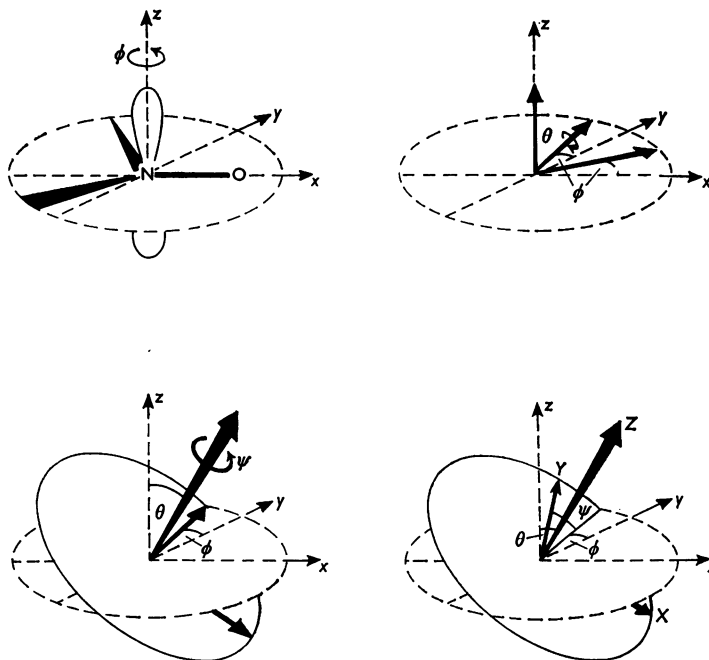


Fig. 2. Illustration of the transformation between two different co-ordinate systems

The nitroxide co-ordinate set (xyz) is transformed into a general co-ordinate set (XYZ) by means of three successive rotations defined by the angles ϕ , θ and ψ . The transformation matrix (T) is:

$$\begin{pmatrix} \cos\theta\cos\phi\cos\psi - \sin\phi\sin\psi, & \cos\theta\sin\phi\cos\psi + \cos\phi\sin\psi, & -\sin\theta\cos\psi \\ -\cos\theta\cos\phi\sin\psi - \sin\phi\cos\psi, & -\cos\theta\sin\phi\sin\psi + \cos\phi\cos\psi, & \sin\theta\sin\psi \\ \sin\theta\cos\phi, & \sin\theta\sin\phi, & \cos\theta \end{pmatrix}$$

relative to the protein to be related to the co-ordinate system of the nitroxide radical.

The A tensor can be expressed as a 3×3 matrix in the co-ordinate system of the nitroxide radical (x, y, z), A_{xyz} . The fast oscillation about a bond of the spin-labelled molecule is described in another co-ordinate system (X, Y, Z). The axis of rotation is the Z -axis of the 'molecular' set, and the problem is to calculate the averaged components of the tensor $A_{XYZ}(\langle A \rangle)$, given A_{xyz} .

The relationship between the two co-ordinate sets can be described by the three Euler angles (ϕ , θ , ψ), and Fig. 2 shows the transformation of the xyz system into the XYZ system in terms of these angles. The matrix representing this rotational transformation T , where $A_{XYZ} = T A_{xyz} \tilde{T}$, is also shown (where $\tilde{}$ indicates transpose). From this equation (Van *et al.*, 1974) the motionally averaged matrix elements of the A_{xyz} (or $\langle A \rangle$) matrix can be calculated by substituting the Euler angles ϕ and θ into T . The motional averaging is performed by calculating the normalized integrals of the angular functions involving ψ over the amplitude of the restricted (or full)

rotation. This is because the Euler angle corresponds to rotation about the Z co-ordinate axis. The normalized integrals required are: $\langle \cos^2\psi \rangle = \int_{-\alpha}^{\alpha} \cos^2\psi d\psi / \int_{-\alpha}^{\alpha} d\psi = \frac{1}{2}(1 + \sin\alpha \cos\alpha/\alpha)$, $\langle \cos\psi \rangle = \sin\alpha/\alpha$ and $\langle \cos\psi \sin\psi \rangle = \langle \sin\psi \rangle = 0$, where α is the half-amplitude of the oscillation or restricted rotation given in Tables 2 and 3. In general, the resulting $\langle A_{xyz} \rangle$ matrix will not be diagonal, although for a full rotation ($\alpha = 180^\circ$) the matrix will be diagonal. After diagonalization, the principal values A_{xx} , A_{yy} and A_{zz} (given in Tables 2 and 3) correspond to the extrema observed in the hyperfine splittings of the spin-labelled haptens. The largest principal value will correspond to the outer splitting, $2A_{z'z'}$, observed in the e.s.r. spectrum of the bound spin-labelled hapten, and thus reflects the motion of the spin label in the combining site.

Effect of polarity on the e.s.r. spectrum

Although the motion of a spin label may average the components of the A tensor and leave the magnitude of A unchanged, this magnitude is affected

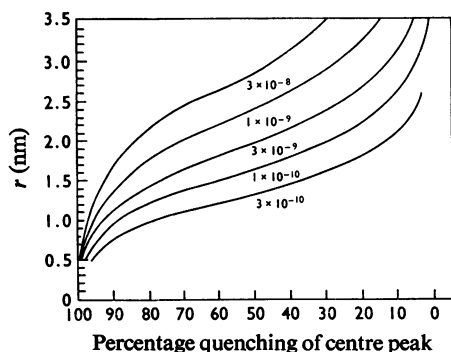
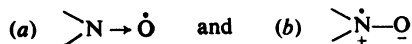


Fig. 3. Distance-dependence of the paramagnetic quenching of the e.s.r. spectrum of a nitroxide radical

The distance (nm) between Gd(III) and the nitroxide group as a function of the height of the central peak for different values of the correlation time τ (s) calculated from eq. (1).

by the environment of the nitroxide group. The hyperfine coupling depends on the unpaired electron-spin density at the nitrogen atom, and, by considering the electronic structure of the nitroxide radical to be represented by the two canonical forms:



it follows that, the more polar the environment, the nearer the structure approaches to that of canonical form (b) and therefore the larger the magnitude of tensor A .

The isotropic-splitting constant A_0 is an index of polarity and is defined by:

$$A_0 = \frac{1}{3} (A_{xx} + A_{yy} + A_{zz})$$

If the spin label is undergoing isotropic motion, A_0 can be measured directly from the three-line spectrum, but if not A_0 may be calculated from the principal values, provided that these can be measured. For an immobilized spin, only A_{zz} can be measured, and an empirical correlation between A_{zz} and A_0 must be used (Griffith *et al.*, 1974).

Attempts have been made to quantify the variation in A_0 in terms of polarity (Seelig *et al.*, 1972; Griffith *et al.*, 1974). Estimates of the electric-field gradient along the axis of the N–O bond sufficient to cause a change in A_0 of 0.04 mT have been made at 10^8 and 10^9 V/m respectively by these authors, the value depending mainly on the choice of the effective molecular radius of the nitroxide radical in solution. For a single positive charge at a distance r from the nitroxide bond in a medium of dielectric constant ϵ :

$$r \text{ (nm)} = (5.0 \pm 2.6)(\cos\theta/\epsilon\Delta A_0)^{\frac{1}{2}}$$

where ΔA_0 (mT) is the change in A_0 induced by the charge, and θ is the angle between the vector r and the N–O bond. The error in the multiplicative factor represents the uncertainty in the calibration of the field-dependence of A_0 arising from the two different estimates of the molecular volume.

In water ($\epsilon = 80$) a positive charge would have to be 0.1–0.3 nm along the axis of the N–O bond to cause a change in A_0 of 0.08 mT (about 0.2 mT in A_{zz}). Polarity effects on the components of the A tensor are, therefore, relatively small compared with the effects of motional averaging. In a hydrocarbon environment, the effects of polarity can be up to a factor of 4 greater. Therefore it will be assumed in the following analysis that the large differences between the experimental A_{zz} values (Table 4) are a consequence of different motional averaging for the various spin labels. If polarity effects could account for these differences, a correlation would be expected between the length of the spin-labelled haptens and their A_{zz} values, since the environment of the nitroxide group would vary between that characteristic of the combining site and that free in solution; this is clearly not the case, as Table 1 shows. A polarity effect will only be considered in cases where motional averaging cannot account for the observed differences.

Distance calculations between a paramagnetic metal ion and a spin label

The dipolar interaction between a paramagnetic ion and a spin label results in a quenching of the e.s.r. spectrum (Taylor *et al.*, 1969). The theory (Leigh, 1970) requires the two spins to be fixed relative to one another and that the time-dependence of the interaction (characterized by the correlation time τ) is dominated by the electron-spin relaxation time of the paramagnetic ion. The dipolar-interaction coefficient C is given by:

$$C = g\beta\mu^2\tau/\hbar r^6 \quad (1)$$

where μ is the magnetic moment of the paramagnetic ion, β the Bohr magneton and r the distance between spin label and metal. C can be related to the quenching of the spectrum and therefore r can be calculated if τ is known (Fig. 3). If the spin label is not rigidly immobilized relative to the paramagnetic ion the theory breaks down, but, since any motion will decrease the dipolar interaction, the calculated distance is an upper limit (Dwek, 1973).

Results and Discussion

Conformational analysis

The six-membered nitroxide rings can undergo flexing between various conformations (Dwek *et al.*, 1975b), and some of these are shown in Fig. 4, which

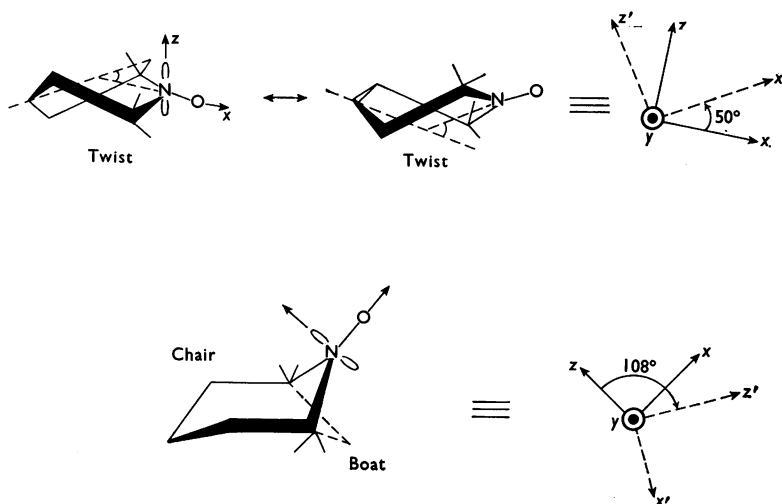


Fig. 4. Flexing in six-membered nitroxide rings

The interconversions between the three conformers of the six-membered nitroxide ring and their equivalence to a rotational transformation are shown.

also demonstrates the equivalence (with respect to the co-ordinate set of the nitroxide groups) between such flexing and a restricted rotation. This rotation can be treated by the rotational-transformation method described above and differs from a previous treatment (Dwek *et al.*, 1975*b*), which considered only the average of the two conformations between which ring-flexing occurred. Although the five-membered nitroxide rings cannot undergo flexing, these haptens, in common with the six-membered nitroxide forms, can undergo restricted bond rotation, and these can also be treated by the rotational-transformation method. The enantiomers of the five-membered nitroxide ring spin labels behave identically, after allowing for the different sign of the angle about the bond of rotation.

The constraints on the torsional angles of the two bonds Dnp-NH, ϕ' , and NH-5(SL), ψ' , for hapten (VI), Dnp-NH-5(SL), are shown in Fig. 5(a). This Figure shows the areas within which there are no unfavourable van der Waals interactions. The number of unfavourable interactions were counted for 10° steps about each bond. Only a few regions of unrestricted motion occur, corresponding to oscillation about the NH-5(SL) bond with the NH group either co-planar with the dinitrophenyl ring or perpendicular to it. As the co-planar conformation has an intramolecular hydrogen bond between the 2-nitro group and the proton on the NH group (Holden & Dickinson, 1969), it is predicted that region I will be by far the most populated. Permitted rotation is then approx. 40° about the NH-5(SL) bond. Fig. 5(b) shows one of the allowed conformations

from region I, for the *R* enantiomer with $\phi' = 0^\circ$, $\psi' = 40^\circ$. Since hydrogen-bond formation is possible even for this hapten, whose motion is so restricted that hydrogen-bonding is least likely to occur, treatment of all subsequent spin labels assumes co-planarity of the Dnp-NH group.

Treatment of the longer hapten (V), Dnp-NH-CH₂-5(SL), was less quantitative, because there is now the possibility of rotation about three bonds. Rotation about CH₂-5(SL) is so restricted that it is considered fixed, and, with the NH-Dnp group held co-planar, there are extensive areas of permitted motion about the NH-CH₂ bond. The main region involves rotations of 40° on each side of the conformation which has the -CH₂- group disposed symmetrically with respect to the plane of the dinitrophenyl ring. There is also a further rotation between 82° and 118° from the same starting conformation. Elsewhere the main unfavourable interactions are between the aromatic ring proton H₍₆₎ and either the protons of the -CH₂- spacer group or one of the methyl groups of the alicyclic ring. Fig. 5(c) shows one of the favourable conformations for the *R* enantiomer, and is the starting conformation already defined.

The absence of a spacer group for hapten (I), Dnp-NH-6(SL), restricts rotation about the NH-6(SL) bond to about 10° , because of steric hindrance between the alicyclic and aromatic rings. Although hapten (II), Dnp-NH-N=6(SL), has an extra atom interposed between the rings, the co-planarity of N-N=C limits rotations to the N-N bond, about which there can be a maximum of 220° rotation.

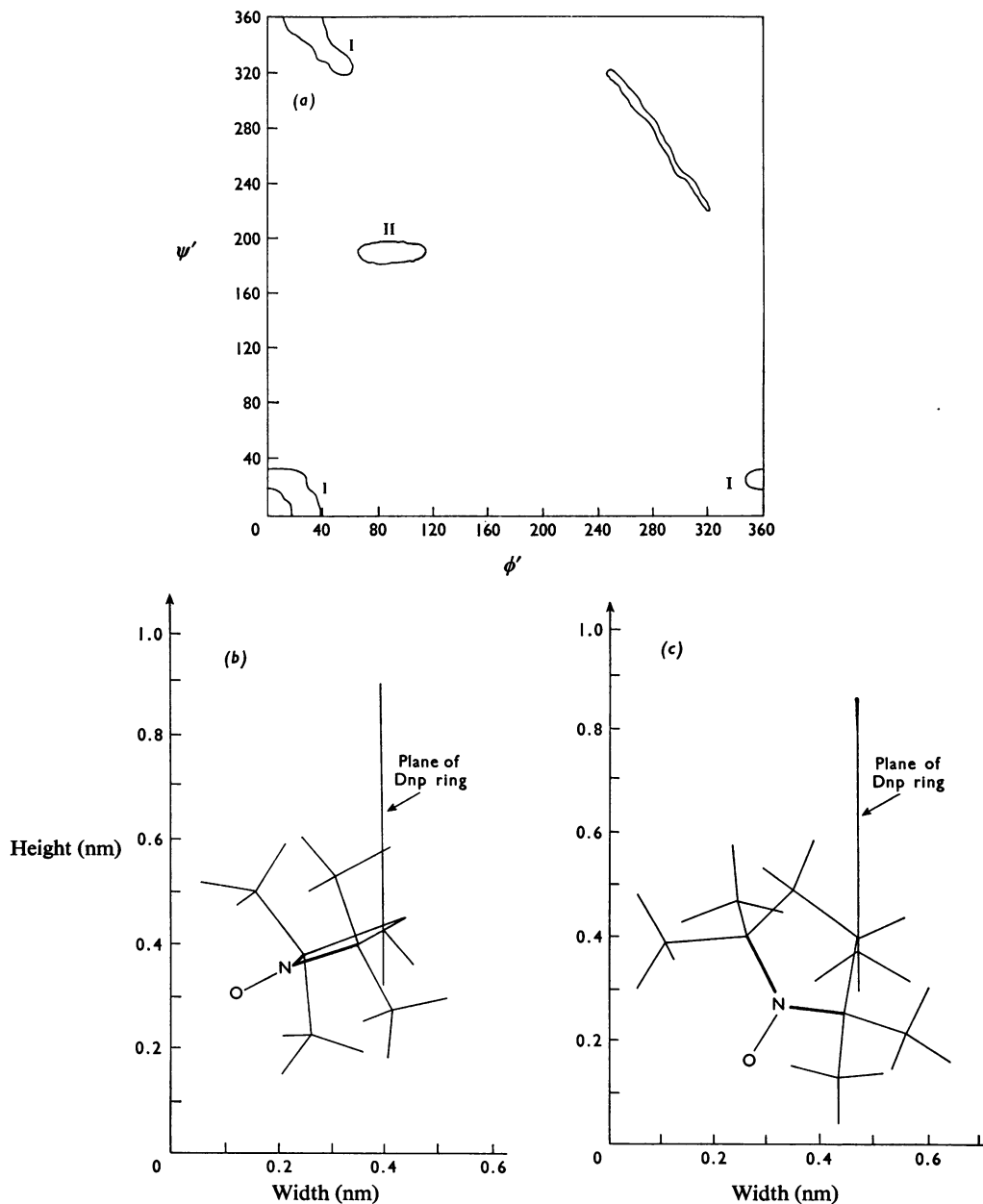


Fig. 5. Stereochemistry of the *R* enantiomers of the two five-membered nitroxide-ring spin labels used to estimate the lateral dimensions of the combining sites

(a) A plot of the areas (denoted I and II) where there are no non-bonded interactions for the *R* and *S* enantiomers of hapten (VI). ϕ' is the angle about the NH-Dnp bond and ψ' is the angle about the NH-5(SL) bond. ($\phi' = 0^\circ$ corresponds to the NH group co-planar with the aromatic ring and the N-H bond pointing towards the 2-nitro group. $\psi' = 0^\circ$ corresponds to the $C_{(1)}-C_{(2)}$ bond of the nitroxide ring co-planar with the aromatic ring for $\phi' = 0^\circ$.) Area I cuts the $\phi' = 0^\circ$ axis where the NH proton can form a hydrogen bond with the 2-nitro group. Area II cuts the $\phi' = 90^\circ$ line where the NH bond is perpendicular to the dinitrophenyl ring and no hydrogen bond can form. (b) and (c) show the stereochemistry of the *R* enantiomers of haptens (VI) and (V) respectively.

Hapten (III), Dnp-NH-CH₂-CO-O-6(SL), now has sufficient spacer groups to permit full rotation about two bonds, O-6(SL) and CO-O, without the two rings coming too close to one another. However, the bulk of the carbonyl interacting with the methylene protons hinders full rotation about the CH₂-CO bond. Finally, for hapten (IV), Dnp-NH-[CH₂]₃-CO-O-6(SL), there is also the possibility of inter-conversion of the conformers of the alicyclic ring.

The results of this analysis, the Euler angles relating these motions to the nitroxide radical itself, the calculations of the principal values of the averaged A tensor and the spatial requirements for the motions, are presented in Tables 1 and 2. These Tables are of general applicability for any Dnp-binding protein (Willan *et al.*, 1977).

Allowance for slow isotropic tumbling

The Stokes-Einstein equation (Dwek *et al.*, 1975b) can provide values of τ for the whole IgA, and the Fab and Fv fragments. From these, the expected changes in $A_{z'z'}$ on changing from fragment Fv to IgA can be calculated (McCalley *et al.*, 1972; Shimshick & McConnell, 1972), assuming isotropic tumbling and immobilization of the spin label relative to the protein. These are presented in Table 3, which gives the ratios of $A_{z'z'}$ between the fragments, assuming a value of 3.2 mT for the rigid limit of this system when there is no molecular tumbling. The actual value for this system is unknown and will depend on the particular environment of the immobilized spin label. The incremental changes in $A_{z'z'}$ given in Table 3 are valid for $A_{z'z'}$ (rigid-limit) values between 3.0 mT and 3.4 mT (McCalley *et al.*, 1972), the range within which the actual value will fall (see below).

By applying the Stokes-Einstein equation to the Fv fragment, it is predicted that $A_{z'z'}$ for a rigid system is 1.17 times as large as the corresponding $A_{z'z'}$ value for the Fv fragment. Values of $A_{z'z'}$ for IgA and the Fab fragment lie between these two extremes, but the non-spherical shapes of these molecules and the possibility of domain motion make the calculated ratios (column six, Table 3) uncertain, in view of the assumption of isotropic tumbling.

Ratios derived from the experimental $A_{z'z'}$ values for three haptens are given in Table 3, and are expressed relative to the Fv fragment. Two of these haptens are known to have little or no motion relative to the protein (see below), and so the different $A_{z'z'}$ values reflect the different tumbling times of the protein fragments. The values for IgA and fragment Fab do not agree with the calculated values, indicating anisotropy in the tumbling and/or domain motion. However, the three different haptens give consistent results, and the mean values of these ratios (1.00:1.05:1.07) are used to allow for the effect of slow tumbling, by correcting each

observed value to that expected in the limit of no tumbling.

It is now possible to relate the calculated hyperfine-splitting constants given in Tables 1 and 2 to the experimentally observed values of Tables 4 and 5. After allowance for the effect of slow molecular tumbling has been made, the experimental $A_{z'z'}$ value may be compared with the largest of the calculated principal values of the motionally averaged A tensor (A_{xx} , A_{yy} or A_{zz}) for the hapten in question (Table 1 or 2). Consequently the motion (or at least limits to the motion) causing the averaging may be inferred, together with the spatial requirements for that motion. From these dimensions a picture of the combining site can be constructed.

Analysis of the six-membered nitroxide ring spin-labelled haptens

The mobility analysis has been discussed previously (Dwek *et al.*, 1975b), giving a depth of 1.1–1.2 nm and approximate lateral dimensions of 0.6 nm × 0.9 nm. One extra hapten (III) is considered here and the result is consistent with the previous conclusions.

Analysis of the five-membered nitroxide ring spin-labelled haptens

The spectra from haptens (V) and (VI) bound to IgA (Fig. 6) not only indicate strong immobilization, but each shows two bound signals due to the two enantiomers (Wong *et al.*, 1974). $A_{z'z'}$ values for all four bound signals are higher than for any member of the six-membered nitroxide ring spin-label series (Table 4), but, of each pair of values, one is significantly greater than the other. The larger referred to as the 'rigid' and the smaller as the 'mobile' enantiomer (Table 5). The lengths of the two haptens from the oxygen atom of the 4-nitro group to the nitroxide bond are 1.1 nm and 0.9 nm for haptens (V) and (VI) respectively, placing them both within the site but with hapten (V) probing the edge.

The identical $A_{z'z'}$ values for hapten (VI) and for the same hapten without the fluorine atom (Wong *et al.*, 1974), and the ability to displace the hapten (VI) with lanthanides, show that the protein is not reacting with the hapten.

Results from different fragments

The two bound signals of hapten (VI) bound to different immunoglobulin fragments are illustrated in Fig. 6. The 'mobile' signal changes little, and the 'rigid' one varies with the fragment. Table 5 shows that hapten (V) behaves similarly. The 'mobile' enantiomer does not sense the slow tumbling of the whole fragment, and the signal is the same for IgA and

Table 1. Information from e.s.r. studies over a series of six-membered nitroxide ring spin-labelled haptens

The Table demonstrates the averaging of the A tensor as a result of molecular motion, and the spatial requirements for this motion. The dimensions of width, height and depth may be related to the picture of the combining site (Fig. 7).

Rigidly immobilized label	Hapten	Motion	Euler angles (degrees)			Principal values of A tensor (mT)			Requirements for motion (nm)		
			ϕ	θ	ψ	A_{xx}	A_{yy}	A_{zz}	Width	Height	Depth
(I) Dnp-NH-		None	90	90	± 25	0.60	0.60	3.20	0.6	0.9	>0.9
		Twist \leftrightarrow twist	90	90	± 54	3.05	0.75	0.60	0.6	0.9	>0.9
		Chair \leftrightarrow boat	0	144	± 180	2.55	1.25	0.60	0.7	0.9	>0.9
		Full rotation at N-C				1.06	1.06	2.29	0.7	0.9	>0.9
		Chair \leftrightarrow boat and full rotation			as above	1.15	1.15	2.10	0.7	0.9	>0.9
(II) Dnp-NH-		Twist \leftrightarrow twist	0	90	± 30	2.99	0.81	0.60	0.6	0.9	—
		Chair \leftrightarrow boat	90	90	± 60	2.45	1.35	0.60	0.6	0.9	—
		Full rotation at N-N (chair)	60	90	± 180	1.90	1.90	0.60	1.1	0.9	1.1
		Full rotation at N-N (twist)	60	65	± 180	1.67	1.67	1.07	1.1	0.9	1.1
		Full rotation at N-N (boat)	60	20	± 180	0.76	0.76	2.89	1.1	0.9	1.1
(III) Dnp-NH-CH ₂ -CO-O-		Isotropic	—	—	—	1.50	1.50	1.50	—	—	<1.2
(IV) Dnp-NH-[CH ₂] ₃ -CO-O-		Isotropic	—	—	—	1.50	1.50	1.50	—	—	<1.5

Table 2. *Information from e.s.r. studies of five-membered nitroxide ring spin-labelled haptens*

The Table demonstrates the averaging of the A tensor as a result of molecular motion, and the spatial requirements of this motion. The restricted rotation is estimated from the conformational analysis. Full bond rotation is also considered, as a theoretical limit. The dimensions of width, height and depth may be related to the picture of the combining site (Fig. 7). Euler angles and requirements for motion were deduced from molecular models.

Hapten	Rotational motion	Euler angles (degrees)			Principal values of A tensor (mT)			Requirements for motion (nm)		
		ϕ	θ	ψ	A_{xx}	A_{yy}	A_{zz}	Width	Height	Depth
(V) Dnp-NH-CH ₂ -N-O 	Restricted Full	0 0	90 90	± 40 ± 180	2.81 1.90	0.99 1.90	0.60 0.60	0.7 0.8	1.0 1.0	1.0 1.0
(VI) 5-F-Dnp-NH-N-O 	Restricted Full	35 35	35 35	± 20 ± 180	0.6 1.02	0.7 1.02	3.10 2.34	0.6 0.7	0.9 1.0	0.8 0.8
(VII) Dnp-NH-N-O 	Restricted Full	20 20	90 90	± 20 ± 180	3.10 1.90	0.70 1.90	0.60 0.60	0.9 1.1	0.8 0.9	1.1 1.1

* Denotes chiral centre.

Table 3. Comparison of the variation in the value of $2A_{z'z'}$ expected for a spin label rigidly bound to the three antibody fragments and undergoing isotropic tumbling, with the experimental results for three bound haptens

Fragment	Mol.wt.	$10^8 \times \tau_r$ (Stokes) (s)	$2\Delta A_{z'z'}$ (mT)	$2A_{z'z'}^*$ (mT)	$A_{z'z'}/A_{z'z'}^*$ (fragment Fv)			
					Calculated	Hapten (I)†	Hapten (V)	Hapten (VI)
Fv	25000	0.7	0.91	5.49	1.00	1.00	1.00	1.00
Fab	50000	1.5	0.53	5.87	1.07	1.05	1.04	1.05
IgA	170000	4.4	0.25	6.15	1.12	1.06	1.06	1.08
Rigid			0.00	6.40	1.17	—	—	—

* This assumes an arbitrary choice of 6.40 mT for the rigid system (Griffith *et al.*, 1965).

† Based on data of Dwek *et al.* (1975b).

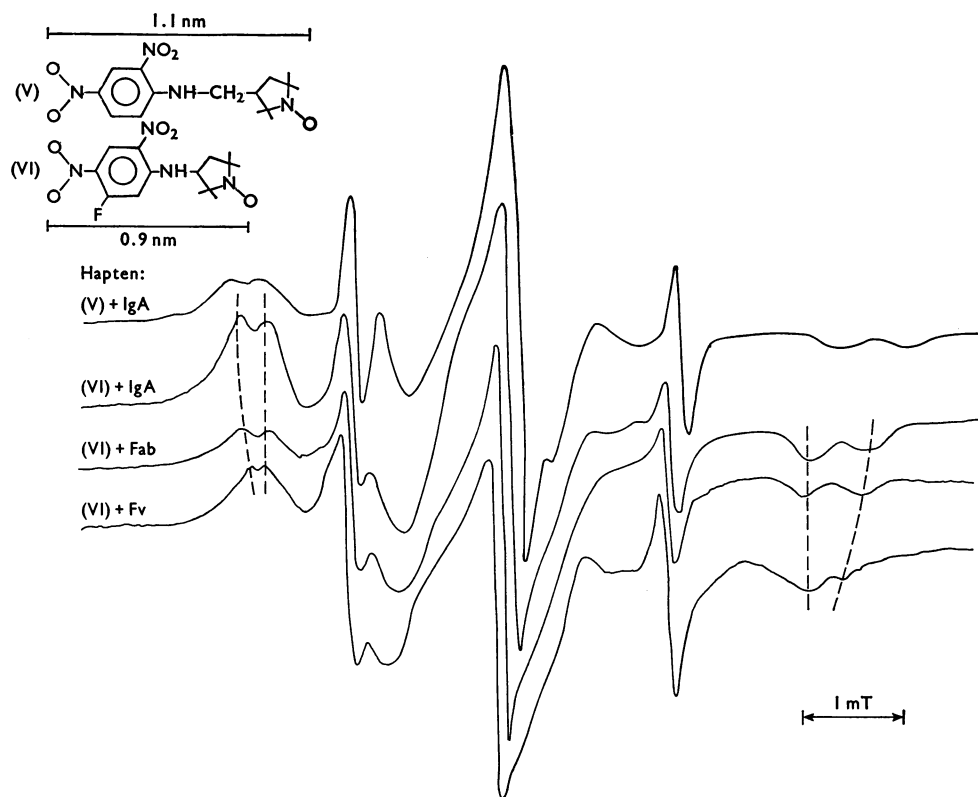
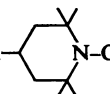
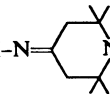
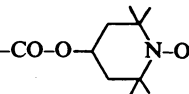
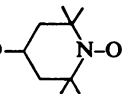
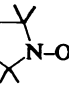
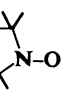
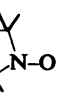


Fig. 6. E.s.r. spectra of haptens (V) and (VI) bound to protein MOPC 315 IgA and its fragments Fab and Fv. In each case the protein concentration was $100 \mu\text{M}$, and spin-label concentration $30 \mu\text{M}$ in $0.05 \text{ M-Pipes}/0.15 \text{ M-NaCl}$, pH 6.4. $T = 20^\circ\text{C}$. Modulation = 0.2 mT .

fragments Fab and Fv, whereas the signal from the other enantiomer, rigidly immobilized relative to the protein, reflects the different tumbling times of the three fragments. Consequently, for haptens (V) and (VI), only the larger of the two $A_{z'z'}$ values in each case will require allowance for the effect of slow molecular tumbling. This interpretation is supported by a study of hapten binding to another myeloma

protein (MOPC 460) and its fragments, in which the site applies no constraints on the hapten's mobility, and $A_{z'z'}$ is independent of the fragment's size (Willan *et al.*, 1977). The identical values of $A_{z'z'}$ for the mobile enantiomers with the three fragments of protein MOPC 315 imply that all three have identical binding sites. It is not clear why the $A_{z'z'}$ value for the mobile enantiomer of haptens (V) and (VI) is

Table 4. Maximum hyperfine splittings, $A_{z'z'}$ (mT) of spin-labelled haptens bound to fragments of myeloma protein MOPC 315. The asterisk denotes the chiral centre giving rise to the two enantiomeric forms of these haptens, to which the two values for haptens (V) and (VI) refer. The limits are explained in the Materials and Methods section.

Spin-labelled hapten	Fragment of protein MOPC 315	$A_{z'z'}$ (mT)
(I) 	Fab	2.67 ± 0.01
(II) 	Fab	2.30 ± 0.05
(III) 	Fv	1.59 ± 0.10
(IV) 	IgA	1.60 ± 0.02
(V) 	Fab	3.20 ± 0.03 2.85 ± 0.03
(VI) 	Fab	3.00 ± 0.03 2.63 ± 0.03
(VII)† 	IgA	3.12 ± 0.03

† Data of Hsia & Little (1973).

Table 5. Maximum hyperfine splittings, $A_{z'z'}$ (mT), for haptens (V) and (VI)

The maximum hyperfine-splitting constants $A_{z'z'}$ (mT) for haptens (V) and (VI) bound to protein MOPC 315 IgA and fragments Fab and Fv are shown. The pairs of values correspond to the two enantiomers of each hapten. The limits are explained in the Materials and Methods section.

Frag- ment	Hapten (V)		Hapten (VI)	
	Fv	3.08 ± 0.03	2.78 ± 0.03	2.84 ± 0.03
Fab	3.20 ± 0.03	2.85 ± 0.03	3.00 ± 0.03	2.63 ± 0.03
IgA	3.28 ± 0.03	2.85 ± 0.03	3.08 ± 0.03	2.65 ± 0.03

independent of the fragment, and therefore of the tumbling time of the whole protein.

Hapten (I) has an $A_{z'z'}$ value indicative of motional

averaging to at least the same extent (Table 4), owing to ring flexing (Dwek *et al.*, 1975b), yet its e.s.r. spectrum is sensitive to slow tumbling (see Table 3), i.e. to the fragment with which it is combined. The ratios of $A_{z'z'}$ values between the different fragments for hapten (I) are identical with those of rigidly immobilized spin labels (see Table 3), supporting the assumption that the motion relative to the protein is always independent of the motion of the whole complex.

Asymmetry of the combining site

The observation of separate bound signals for the two enantiomers shows that the site must be asymmetric with respect to the plane of the dinitrophenyl ring.

The two enantiomers of hapten (VI) probe different sides of the site with respect to the dinitrophenyl ring

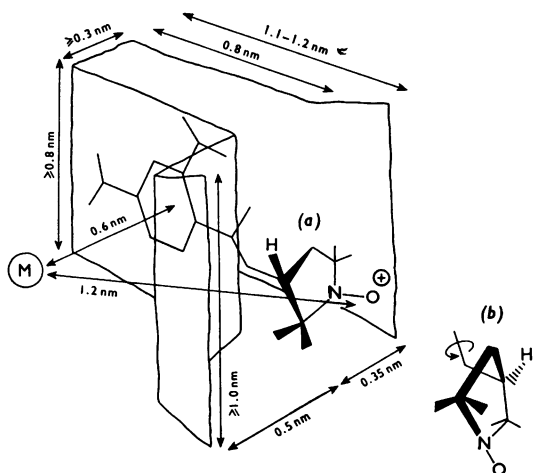


Fig. 7. Combining site of protein MOPC 315 as determined by spin-label mapping

The two enantiomers of haptens (V) are shown, (a) and (b); the former is rigidly immobilized but the latter is free to undergo a restricted rotation as shown. The metal-binding site is also indicated.

because of the restricted mobility of this haptens. The $A_{z'z'}$ values of this haptens are 3.34 mT and 2.65 mT after allowance for molecular tumbling in the former case. The value of 3.34 mT must arise from an essentially immobilized spin label, one showing that side of the site can accommodate the nitroxide ring, but allow no motion. The second value is less than that expected for the restricted rotation through 40° , but larger than that for full rotation (Table 2), setting an upper limit on the dimensions of the other side of the site.

Although haptens (V) has intrinsically greater mobility, the $A_{z'z'}$ values (3.56 mT and 2.85 mT after allowance for tumbling) are all greater than for haptens (VI). Fig. 5(c) shows that this haptens requires more space for its motion, and the fact that it undergoes the restricted rotation of 80° puts a lower limit on the dimensions of the side of the site that allows motion to an enantiomer of haptens (VI). The other side has, as expected, the same effect on haptens (V) and (VI).

The $A_{z'z'}$ value of haptens (VII), after correction for tumbling is 3.42 mT, indicating full immobilization, but since the label itself has little intrinsic mobility this value may only reflect the rigidly held dinitrophenyl ring and so this does not provide any further information about the site.

The lateral dimensions of the combining site required to accommodate the motion of the mobile enantiomers of both haptens (V) and (VI) is 0.7 nm (Table 2), 0.5 nm of which must lie to one side of the plane defined by the dinitrophenyl ring (Figs. 5b and 5c). On the other side of the combining site,

0.3–0.4 nm is required to accommodate the rigidly held enantiomers. In this way, by using the results in Tables 4 and 5, with the results of the conformational analysis of the haptens, a picture of the combining site is built up (Fig. 7).

Polarity profile of the combining site

Since the polarity of the environment of the nitroxide radical can affect the magnitude of the A tensor and consequently the observable $A_{z'z'}$, the magnitude of this effect is important to the previous mobility analysis. It has been suggested that differences in $A_{z'z'}$ between haptens bound to an antibody-combining site may be due entirely to polarity variations (Wong *et al.*, 1974).

Two effects are important in considering polarity of the combining site: the exclusion of water so that the dielectric constant within the site is decreased, and the electric-field effects of polar residues. The first effect is small, as shown by the fact, that between an aqueous and a totally hydrocarbon environment, $A_{z'z'}$ only changes by 0.2–0.3 mT at most (Griffith *et al.*, 1974). The second effect is also small, as shown by the calculation in the Theory section. These changes may be compared with the larger variations in $A_{z'z'}$ for which mobility arguments alone can account.

There is, however, a relatively large difference in the $A_{z'z'}$ values between the 'rigid' enantiomers of haptens (V) and (VI): $3.56 - 3.34 = 0.22$ mT after correction for slow tumbling (Table 5). Since neither has any motion, this difference must be due to a polarity effect, for example, a nearby charged amino acid residue. The nitroxide group of haptens (V) is 1.1 nm from the back of the site, is rigidly immobilized and probes the edge of the site where the dielectric constant is probably similar to that of water. The environment of the nitroxide group of haptens (VI) 0.2 nm inside the site, is unlikely to be very different, and is unable to account for the different $A_{z'z'}$ value, unless it is assumed that the nitroxide of haptens (V) is close to a positive charge, which results in its $A_{z'z'}$ value being unusually high. A charge 0.1–0.2 nm away could account for a difference in $A_{z'z'}$ of 0.2 mT. The effect of this charge on haptens (VI), which is 0.2 nm further away, is less than one-quarter of that on haptens (V) as a result of the inverse-square law (Griffith *et al.*, 1974). The geometry of haptens (V) allows the positive charge to be placed as shown in Fig. 7. Independent evidence in support of a positive charge at this location in the combining site comes from the perturbation of the pK_a values of phosphate and phosphonate derivatives of dinitrophenyl (Wain-Hobson *et al.*, 1977).

The polarity index A_0 may be calculated for the different haptens to provide a polarity profile of the combining site. The calculated values of A_0 are presented in Table 6, and in Fig. 8 they are corre-

Table 6. Values of A_0 obtained for different spin labels

The values of the isotropic hyperfine-splitting constant A_0 (the polarity index) for the various haptens used to form the polarity profile shown in Fig. 8. The limits are explained in the Materials and Methods section.

Hapten	A_0 (mT)	Method of calculation (refer to the text)
(II)	1.55 ± 0.01	$A_0 = \frac{1}{3}(2A_{x'x'} + A_{z'z'})$
(III)	1.59 ± 0.1	Isotropic spectrum
(IV)	1.60 ± 0.02	Isotropic spectrum
(V) ('rigid' enantiomer)	1.49 ± 0.01	Correlation with $A_{z'z'}$
(VI) ('rigid' enantiomer)	1.40 ± 0.01	Correlation with $A_{z'z'}$
Free spin label	1.68 ± 0.01	Isotropic spectrum

lated with the combining site of the fragment, described in terms of subsites of interaction provided by temperature-jump kinetic mapping studies (Haselkorn *et al.*, 1974). The correlation is good, particularly for the positive subsite S_4 .

The above analysis of the experimental results depends on the relative magnitudes of the effects of motional averaging and polarity on the e.s.r. spectrum, particularly since the 'rigid-limit' value of $A_{z'z'}$ for this system is unknown. The application of the terms 'rigid' and 'mobile' in previous sections to the enantiomers of haptens (V) and (VI) may be justified as follows.

After correction for the effect of slow tumbling in those enantiomers sensitive to changing fragment, the difference in the $A_{z'z'}$ values between the two enantiomers for both haptens (V) and (VI) is 0.7 mT. This can only be accounted for in terms of a difference in mobility. However, the difference between the two higher values of these haptens is 0.2 mT. This can be accounted for by either a polarity or a motional averaging effect. For motional averaging the value 3.56 mT [hapten (V)] would then be the 'rigid-limit' value and the $A_{z'z'}$ value of 3.34 mT for hapten (VI) would indicate some motion. This means that the combining site must immobilize the longer and inherently more flexible hapten (V), but allowing motion of the corresponding enantiomer of the shorter hapten (VI), which requires more space (Figs. 5b and 5c). Such an interpretation is not feasible, and the difference of 0.2 mT must therefore result from a polarity effect. The 'rigid limit' must be close to 3.34 mT and, in view of the other results [e.g. hapten (VII), Table 4], may be nearer 3.4 mT, within the limits placed on the arbitrary choice of 3.2 mT considered above.

Furthermore the method assumes that the restrictions on the motions of the spin labels are determined by the shape of the combining site and not

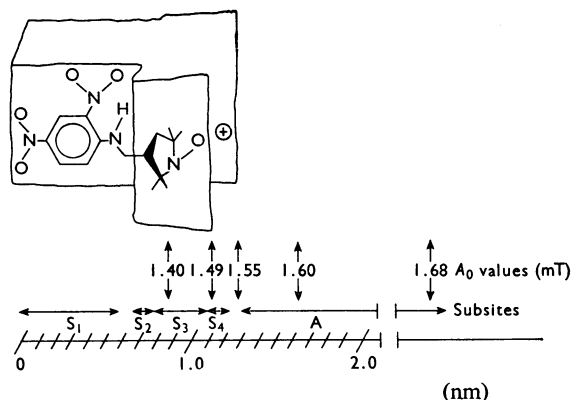


Fig. 8. Polarity profile of the combining site of protein MOPC 315

The profile correlates with the 'subsites of interaction' of Haselkorn *et al.* (1974). S_1 is the first Dnp subsite; S_2 is the first hydrophobic subsite; S_3 is the second hydrophobic subsite; S_4 is the positive subsite; A is the free aqueous environment.

by specific interactions between the protein and the different haptens. In this study there are no marked discontinuities in the e.s.r. spectra between the different haptens, and the binding constants (Willan *et al.*, 1977) show no evidence for such specific interactions.

Lanthanide-binding site

The predominant effect of binding a paramagnetic lanthanide such as Gd(III) on the e.s.r. spectrum of a spin-labelled hapten bound to a protein is a decrease in the intensity of the bound signal. This may be interpreted in terms of the quenching theory described above. For the Fv fragment of protein MOPC 315, however, the lanthanide and hapten sites interact (Dwek *et al.*, 1976). The binding of metal may cause a change in the combining site, affecting the mobility of the spin label, or displace it, either of which effects might result in a loss of intensity of the bound signal. La(III) is used as a control for any non-paramagnetic effects. Only the quenching of Gd(III) over and above that caused by La(III) is attributed to the paramagnetic quenching from which the distance calculations can be made.

On binding metal, an increase in the signal from free spin label is observed, with only a slight increase, in the hyperfine-splitting constant $A_{z'z'}$ for the bound signal (<0.01 mT). This confirms that the displacement of hapten from the combining site is probably the main cause of the quenching by La(III). The effects of metal binding are illustrated by hapten (VI) (Fig. 9), which shows two bound signals corresponding to the two enantiomers. The addition of

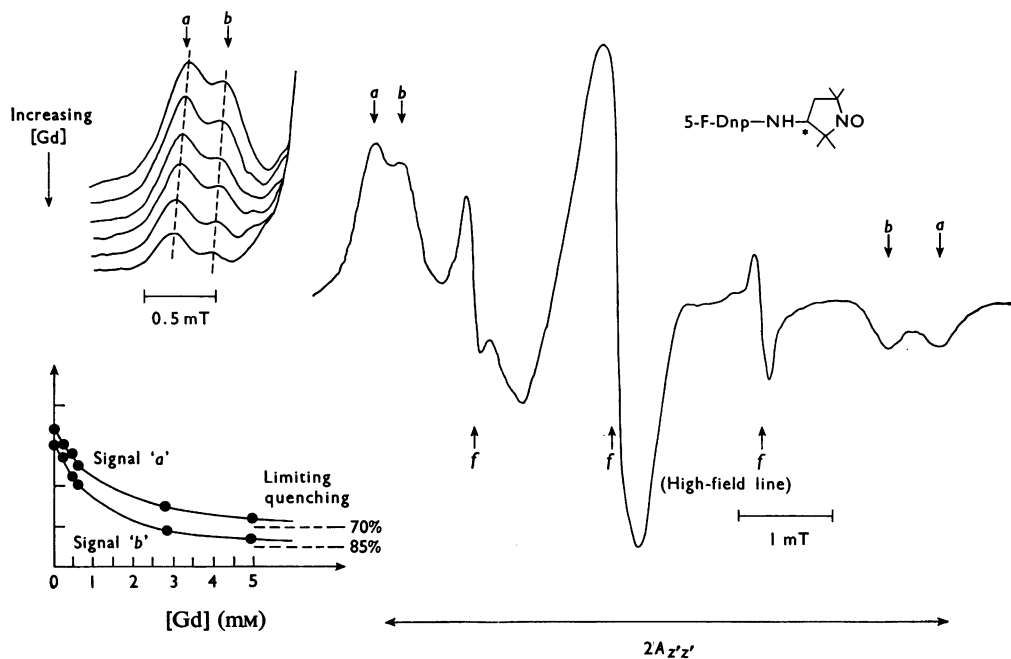


Fig. 9. E.s.r. spectrum of hapten (VI) bound to protein MOPC 315 IgA showing the bound signals (a and b) of the two enantiomers. The positions of the peaks contributed by free spin label are shown (f), and the insets show the effect of Gd(III) addition on the bound signals (a and b). Conditions were as for Fig. 6.

Gd(III) quenches the two bound signals differently (upper inset, Fig. 9), and the limiting quenchings are estimated from a plot of peak height against metal concentration (lower inset, Fig. 9). A slight change in $A_{z'z'}$ is also detected as metal is added (upper inset, Fig. 9), and, since this is observed for the rigidly bound enantiomer, it must be due to a change in the polarity of the environment of the nitroxide radical rather than the mobility of the label.

The results of La(III) and Gd(III) titrations with spin-labelled haptens (I), (II), (V) and (VI) are presented in Table 7, with the metal-nitroxide distances calculated for two values of the correlation time τ , which represent the likely range for τ in the system (Burton *et al.*, 1977). The differential quenching of the two bound peaks of haptens (V) and (VI) means that one enantiomer is nearer the metal than the other, and in each case it is the 'rigid' enantiomer that is further away.

All the results in Table 7 were obtained with IgA molecules, since the separation of the two bound signals, corresponding to the two enantiomers, is greatest in this case (see Fig. 6). Although the Fab and Fv fragments were also used and gave identical results, the uncertainties were larger because of the overlapping peaks. Titrations with Gd(III) are complicated by the superposition of the e.s.r. signal of the ion itself, and those with both La(III) and

Gd(III) by the increasing free spin label as hapten is displaced. The high-field line of the free spectrum is the best measure of displacement, since the bound spectrum contributes little to this region. The use of La(III) as a control is justified, since it causes the same final amount of displacement as Gd(III).

Location of the lanthanide-binding site

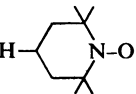
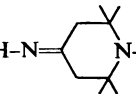
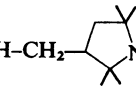
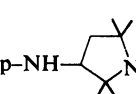
Four independent determinations of the metal-to-nitroxide distance suffice to locate the metal site uniquely. Since the positions of the nitroxide groups can be related to the dinitrophenyl ring through the known molecular geometries of the haptens, the metal is located relative to the ring. Not all of the distances calculated are equally reliable, partly because the distance can only be regarded as an upper limit for those labels undergoing some motion. In these cases the position of the nitroxide group cannot be defined accurately. There are only three distances which are sufficiently accurate to be used.

Taking the metal-nitroxide distances for the 'rigid' enantiomers of haptens (V) and (VI), and the 'mobile' enantiomer of hapten (V) (which undergoes only a very restricted rotation), three equations of the form:

$$r^2 = (x-a)^2 + (y-b)^2 + (z-c)^2$$

Table 7. Limiting values of the lanthanide quenching of nitroxide ring spin-label e.s.r. spectra

The limiting quenching (% decrease of initial peak intensity) caused by Gd(III) and La(III) for various haptens bound to protein MOPC 315 IgA. Metal to nitroxide distances (nm) are calculated for the two values of the correlation times which represent the possible limits for the system (Burton *et al.*, 1977). The limits are explained in the Materials and Methods section.

Hapten	Limiting quenching (%)		Distance (nm)		
	Gd(III)	La(III)	$\tau_c = 10^{-9}$ s	$\tau_c = 10^{-10}$ s	
(I) 	70 ± 2	45 ± 2	1.65 ± 0.05	1.10 ± 0.05	
(II) 	95–100	70–80	<1.2	<0.8	
(V) 	'Rigid'	60 ± 2	35 ± 2	1.75 ± 0.05	1.20 ± 0.05
	'Mobile'	75 ± 2	50 ± 2	1.60 ± 0.05	1.10 ± 0.05
(VI) 	'Rigid'	70 ± 2	40 ± 2	1.60 ± 0.05	1.10 ± 0.05
	'Mobile'	82 ± 2	48 ± 2	1.45 ± 0.05	1.00 ± 0.05

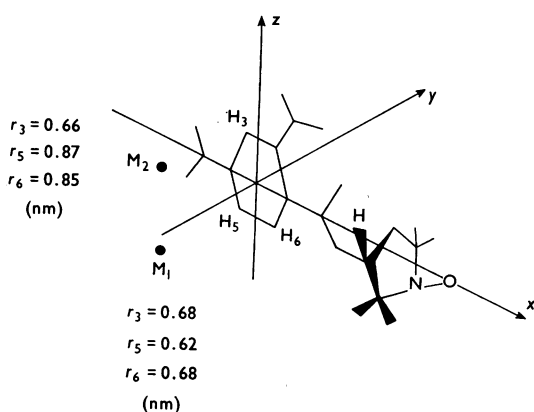
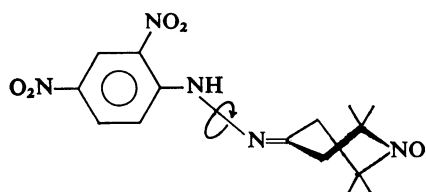


Fig. 10. Positioning the metal-binding site by e.s.r. The two possible positions for the metal-binding site (M_1 and M_2) located by e.s.r. relative to the dinitrophenyl ring. The distances from these two sites to the three protons of the ring are shown (nm).

ring, as shown in Fig. 10. Simultaneous solution of these equations provides two points, which are shown in Fig. 10, the metal-nitroxide distances corresponding to $\tau = 10^{-10}$ s being used. The metal-proton distances for the three ring protons expected for each of the two metal sites are also shown. The result depends critically on knowing the positions of the three nitroxide groups, and, since there is uncertainty in these (perhaps as much as 0.1 nm in each direction for the 'mobile' enantiomer), it cannot be considered a precise location of the metal site. The many variables (three co-ordinates for each nitroxide, and the three metal-nitroxide distances) make it very difficult to estimate the error in these positions. The three metal-nitroxide distances calculated on the basis of $\tau = 10^{-9}$ s gave no real simultaneous solution. This may mean that such a value for τ is unreasonable and suggests that the upper limit of $\tau = 10^{-10}$ s (Burton *et al.*, 1977) may be a more realistic value. This does not change the relative values of the distances.

Fig. 10 shows that one of the solutions lies below the x - y plane and the other above, and so it may be possible to distinguish between these by considering the unusual result for hapten (II) (Table 7). Unlike the other haptens, the nitroxide group of hapten (II) has considerable mobility entirely below this plane,

may be written. r is the metal-nitroxide distance, (x, y, z) the co-ordinates of the metal-binding site and (a, b, c) the position of the nitroxide group in a co-ordinate system centred on the dinitrophenyl



(II)

since rotation can only occur about one bond (see Table 2). The calculated average metal-nitroxide distance is less than 0.8 nm (Table 7) and therefore at some point during its motion the nitroxide group must approach even closer than this. The dependence will weight the average towards the smaller distances. This suggests that the metal site lying below the x - y plane is the more likely of the two. This conclusion is supported by n.m.r. relaxation studies (see below), which show that the metal must be equidistant from all three protons. This is only true for the 'lower' position (M_1) in Fig. 10.

The metal-binding site, as determined by paramagnetic relaxation of spin labels, has been included in Fig. 7. It lies roughly on the 6-fold rotation axis of the dinitrophenyl ring at a distance of 0.6 nm, on the side further from the positive charge and the immobilized enantiomers of haptens (V) and (VI). The metal-nitroxide distances for haptens not used to locate the site (Table 7) are consistent with this position for the metal.

Proton n.m.r. relaxation studies (at 270 MHz) on dinitrobenzene solutions in the presence of fragment Fv/Gd(III)

An independent method for locating the metal-binding site relative to the haptent is from the nuclear-relaxation rates of the three dinitrophenyl protons in the presence of Gd(III). By using the Solomon-Bloembergen equation, the spin-lattice relaxation time can be related to the metal-proton distance if the correlation time is known (Dwek, 1973).

This type of experiment requires that the condition of fast exchange (Dwek, 1973) is fulfilled, which means that the paramagnetic contribution to the relaxation time of the dinitrophenyl protons, termed T_{1M} , must be greater than the lifetime, τ_M , of the dinitrophenyl in the fragment Fv-Gd-Dnp complex. These quantities are related to the measured paramagnetic contribution to the relaxation rate $1/T_{1P}$ and the fraction, P_M of dinitrophenyl ligand bound to the fragment Fv-Gd(III) complex by the equation:

$$\frac{1}{P_M T_{1P}} = \frac{1}{T_{1M} + \tau_M}$$

The relationship between the dissociation constant K_D and τ_M (Dwek, 1973) is:

$$\tau_M = \frac{k_{on}}{K_D}$$

where k_{on} is the rate constant for the encounter between antibody and haptent, which has been shown to be a single-step process (Haselkorn *et al.*, 1974; Dwek, 1976) and to be approx. $2 \times 10^8 \text{ s}^{-1}$. The haptent must not itself chelate metal, since the effects of the resulting metal-haptent complexes on the relaxation rates would obscure any additional contributions from the protein. *m*-Dinitrobenzene was therefore chosen as the haptent.

Table 8 lists the relaxation rates of dinitrobenzene protons (1 mM) in a solution of the Fv fragment (200 μM) and Gd(III) or La(III) (200 μM) at pH 6.3. The differences between the solutions containing Gd(III) and La(III) represent the paramagnetic contribution to the relaxation rates, which is very similar for each proton. The weak binding and limited solubility of dinitrobenzene mean that only an estimate of K_D approx. 10^{-4} M can be obtained (Haselkorn *et al.*, 1974). This gives an upper limit for the fraction of dinitrobenzene bound to the fragment Fv-Gd(III) complex of 0.16, on the basis of the known dissociation constant for fragment Fv and Gd(III) (Dwek *et al.*, 1976). This, however, does not take into account any effects of antagonism between metal and ligand sites (Dwek *et al.*, 1976), which could cause a further substantial decrease in the fraction bound. Substituting this value of P_M into the above equation gives the values of $1/(T_{1M} + \tau_M)$ listed in Table 8. Fast-exchange conditions are observed in this system for the dinitrobenzene protons. The use of the Solomon-Bloembergen equation, with a rotational correlation time of $7 \times 10^{-9} \text{ s}$ (Dwek *et al.*, 1975a), results in the distances (r) given in the last column of Table 8. The use of an upper limit of P_M means that these calculated values of r also represent upper limits. The relative distances are almost identical, and this is independent of any assumption as to the fraction bound. These results therefore support the e.s.r. result, which places the metal-binding site approximately equidistant from all three dinitrophenyl protons.

Comparison of data with model-building studies

(a) *E.s.r. data.* In deciding the depth of the combining site given by the molecular model (Padlan *et al.*, 1976), it is essential to postulate a mode of haptent binding, to provide a limit to the region probed by haptens, and thus dimensions comparable with those calculated by experiment. The presence of two nitro groups on the haptent, which are necessary for strong binding, suggest some hydrogen-bonding to amino acid side chains (Haselkorn *et al.*, 1974).

Table 8. Spin-lattice relaxation rates (at 270 MHz) of *m*-dinitrobenzene protons in solutions containing fragment Fv and either Gd(III) or La(III)

Relaxation rates were measured in ²H₂O at 30°C and pH6.3. Solutions contained: Dnp, 1 mM; Fv fragment, 200 μM; M(III), 200 μM. Some 256 scans were collected for each reading. The limits are explained in the Materials and Methods section.

Dinitrobenzene protons	$T_{1\text{obs}}^{-1}$ (s ⁻¹)		T_{1P}^{-1} (s ⁻¹)	$1/(T_{1M} + \tau_M)^*$ (s ⁻¹)	r (nm)†
	Gd(III)	La(III)			
H ₍₃₎	0.70 ± 0.05	0.37 ± 0.05	0.33 ± 0.05	<1.83	<0.84
H ₍₅₎ , H ₍₁₎	0.77 ± 0.05	0.45 ± 0.05	0.32 ± 0.05	<1.78	<0.86
H ₍₆₎	1.00 ± 0.10	0.50 ± 0.10	0.50 ± 0.10	<2.78	<0.79

* Calculated by assuming a fraction bound of ≤0.16.

† From the Solomon-Bloembergen equation by using a rotational correlation time of 7 × 10⁻⁹s (Dwek *et al.*, 1976).

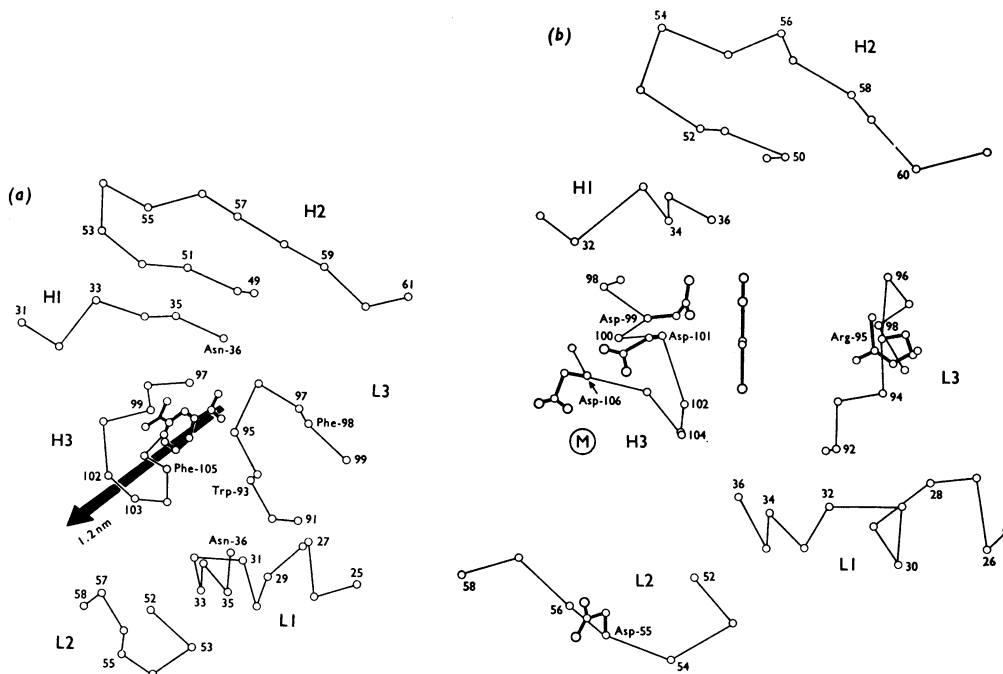


Fig. 11. Predicted combining site of protein MOPC 315

(a) Combining site showing the hypervariable loops of the heavy (H) and light (L) chains (Padlan *et al.*, 1976) and the hapten position relative to the two chains. The view shown is looking into the site at 35° to the plane of the dinitrophenyl ring. The shaded arrow represents the depth of the combining site which is 1.2 nm. (b) A view of the combining site in the plane of the dinitrophenyl ring showing the location of the positive charge (arginine-95), four carboxyl residues (aspartate-99, -101, -106 and -55) and the metal-binding site. The two most likely residues involved in metal binding are aspartate-106 and aspartate-55.

Positioning the dinitrophenyl ring parallel to tryptophan-93_L in the way calculated from n.m.r. studies (Dower *et al.*, 1977) gives a depth of 1.2 nm. Significant variations in the orientation of the tryptophan can be excluded, since they result in a considerably shorter combining site and remove the possibility of hydrogen-bonding to asparagine-36_L.

The width and height vary greatly along the length of the hapten, being smallest around the dinitrophenyl moiety, where dimensions of 0.8 nm × 0.35 nm provide a tight fit for the ring. Because of the asymmetry at the entrance of the combining site and the relative freedom of motion of side chains, it is more difficult to define precisely the dimensions from the

model. The identification of the origin of the positive charge would fix the position of the side chains of either lysine-52_H or arginine-95_L, since they are the only positively charged residues capable of interaction with the haptens. However, with the mode of dinitrophenyl binding mentioned above, it is not possible to distinguish between these two possibilities, nor, more importantly, can the observed differences in mobility of the two enantiomers of hapten (V) be accounted for. From this we conclude that the very bulky side chains of the short spin-labelled haptens affect the exact mode of binding of the dinitrophenyl ring. Thus, if the dinitrophenyl and tryptophan-93_L overlap as required by the n.m.r. results (Dower *et al.*, 1977) and the 4-nitro group can hydrogen-bond to asparagine-36_L, with the 2-nitro group pointing towards H1 rather than L1 (Fig. 11*a*), the conclusions on nitroxide-ring position and mobility, from model-building studies, become consistent with the e.s.r. observations. Furthermore the nitroxide ring then can only interact with arginine-95_L as the source of positive charge.

The e.s.r. mapping determines the structure at low resolution and probes only the rigidity and overall dimensions. In solution the details at atomic resolution can only come from n.m.r. studies.

(b) *Metal-binding data.* Both the n.m.r. and e.s.r. studies suggest that the location of the metal-binding site is 0.7 nm from each of the three dinitrophenyl aromatic protons. Dwek *et al.* (1976) have shown that there are at least two acidic groups involved in chelating the lanthanide. In the model several acidic side chains are suitably placed to act as chelating groups for the model. The two residues most likely to be involved are aspartate-106_H and aspartate-55_L (Fig. 11*b*), and these place the metal site approx. 0.9 nm from each of the dinitrophenyl protons, in reasonable agreement with the experimental results. There are a further two aspartate groups, aspartate-101_H and -99_H, which are not in suitable positions to bond to metal unless there is a conformational change on binding. For aspartate-101_H to bind to metal the whole hypervariable three-loop of the heavy chain (H3) needs to move out from the hapten-binding site, whereas aspartate-99_H points into the site and would thus require a distortion of the loop in its vicinity for bonding to be possible. Either of these processes would affect hapten binding and may be time-dependent. This could account for the observed time-dependent antagonism between metal and hapten (Dwek *et al.*, 1976).

Note Added in Proof (Received 26 April 1977)

The chemical modifications of protein 315 by Klostergaard *et al.* (1977*a,b*) support the conclusion that arginine-95_L is the positively charged residue in the combining site.

We thank Professor R. R. Porter, F.R.S., Professor D. C. Phillips, F.R.S., and Professor R. J. P. Williams, F.R.S., for their encouragement and interest in this work. We also thank the Medical Research Council and the Science Research Council for their support. R. A. D. is a member of the Oxford Enzyme Group. We are grateful to Professor Zeev Luz for his critical comments on the manuscript. D. G. is the recipient of an EMBO short-term fellowship.

References

- Burton, D. R., Forsén, S., Karlstrom, G., Dwek, R. A., McLaughlin, A. C. & Wain-Hobson, S. (1976) *Eur. J. Biochem.* **71**, 519–528
- Dower, S. K., Wain-Hobson, S., Gettins, P., Givol, D., Jackson, W. R. C., Perkins, S. J., Sunderland, C. A., Sutton, B. J., Wright, C. E. & Dwek, R. A. (1977) *Biochem. J.* **165**, 207–225
- Dwek, R. A. (1973) *Nuclear Magnetic Resonance in Biochemistry*, Clarendon Press, Oxford
- Dwek, R. A. (1976) *Contemp. Top. Mol. Immunol.* **6**, 1–53
- Dwek, R. A., Knott, J. C. A., Marsh, D., McLaughlin, A. C., Press, E. M., Price, N. C. & White, A. I. (1975*a*) *Eur. J. Biochem.* **53**, 25–39
- Dwek, R. A., Jones, R., Marsh, D., McLaughlin, A. C., Press, E. M., Price, N. C. & White, A. I. (1975*b*) *Philos. Trans. R. Soc. London Ser. B* **272**, 53–74
- Dwek, R. A., Givol, D., Jones, R., McLaughlin, A. C., Wain-Hobson, S., White, A. I. & Wright, C. (1976) *Biochem. J.* **155**, 37–53
- Freed, J. H. (1976) in *Spin Labelling* (Berliner, L. J., ed.), pp. 53–132, Academic Press, London and New York
- Griffith, O. H., Cornell, D. W. & McConnell, H. M. (1965) *J. Chem. Phys.* **43**, 2909–2910
- Griffith, O. H., Dehlinger, P. J. & Van, S. P. (1974) *J. Membr. Biol.* **15**, 159–192
- Haselkorn, D., Friedman, S., Givol, D. & Pecht, I. (1974) *Biochemistry* **13**, 2210–2222
- Hochman, J., Inbar, D. & Givol, D. (1973) *Biochemistry* **12**, 1130–1135
- Holden, J. R. & Dickinson, C. (1969) *J. Phys. Chem.* **73**, 1199–1203
- Hsia, J. C. C. & Piette, L. H. (1969) *Arch. Biochem. Biophys.* **129**, 296–307
- Hsia, J. C. & Little, J. R. (1973) *FEBS Lett.* **31**, 80–84
- Inbar, D., Hochman, J. & Givol, D. (1972) *Proc. Natl. Acad. Sci. U.S.A.* **69**, 2659–2662
- Klostergaard, J., Grossberg, A. L., Krausz, L. M. & Pressman, D. (1977*a*) *Immunochemistry* **14**, 37–44
- Klostergaard, J., Krausz, L. M., Grossberg, A. L. & Pressman, D. (1977*b*) *Immunochemistry* **14**, 107–110
- Leigh, J. S., Jr. (1970) *J. Chem. Phys.* **52**, 2608–2612
- McCalley, R. C., Shimshick, E. J. & McConnell, H. M. (1972) *Chem. Phys. Lett.* **13**, 115–119
- Padlan, E. A., Davies, D. R., Pecht, I., Givol, D. & Wright, C. E. (1976) *Cold Spring Harbor Symp. Quant. Biol.* **41**, in the press
- Poljak, R. J. (1975) *Adv. Immunol.* **21**, 1–33
- Seelig, J., Limacher, H. & Bader, P. (1972) *J. Am. Chem. Soc.* **94**, 6364–6371

- Shimshick, E. J. & McConnell, H. M. (1972) *Biochem. Biophys. Res. Commun.* **46**, 321-327
- Stryer, L. & Griffith, O. H. (1965) *Proc. Natl. Acad. Sci. U.S.A.* **54**, 1785-1791
- Taylor, J. S., Leigh, J. S., Jr. & Cohn, M. (1969) *Proc. Natl. Acad. Sci. U.S.A.* **64**, 219-226
- Van, S. P., Birrell, G. B. & Griffith, O. H. (1974) *J. Magn. Reson.* **15**, 444-459
- Wain-Hobson, S., Dower, S. K., Gettins, P., Givol, D., McLaughlin, A. C., Pecht, I., Sunderland, C. A. & Dwek, R. A. (1977) *Biochem. J.* **165**, 227-235
- Willan, K. J., Marsh, D., Sunderland, C. A., Sutton, B. J., Wain-Hobson, S. & Dwek, R. A. (1977) *Biochem. J.* **165**, 199-206
- Wong, L. T. L., Piette, L. H., Little, J. R. & Hsia, J. C. (1974) *Immunochemistry* **11**, 377-379